Asynchronous Representation and Processing of Non–stationary Signals in a Time-frequency Context

L. F. Chaparro, E. Sejdić, A. Can, O. Alkishriwo[(1)], S. Şenay [(2)], and A. Akan[(3)]

[(1)]Department of Electrical and Computer Engineering, 1140 Benedum Hall, University of Pittsburgh, Pittsburgh, PA, 15261

[(2)] School of Natural Sciences, University of California, Merced, CA.

[(3)] Dept. of Electrical and Electronics Eng., Istanbul University, Istanbul, Turkey

***Abstract*—Non–stationarity relates to the variation over time of the statistics of a signal. Therefore, signals from practical applications which are realizations of non–stationary processes are difficult to represent and to process. In this paper, we provide a comprehensive discussion of the asynchronous representation and processing of non–stationary signals using a time-frequency framework. Power consumption and type of processing imposed by the size of the devices in many applications motivate the use of asynchronous, rather than conventional synchronous, approaches. This leads to the consideration of non–uniform, signal–dependent level–crossing and asynchronous sigma delta modulator (ASDM) based sampling. Reconstruction from a non–uniform sampled signal is made possible by connecting the sinc and the Prolate Spheroidal Wave (PSW) functions — a more appropriate basis. Two decomposition procedures are considered. One is based on the ASDM that generalizes the Haar wavelet representation and is used for representing analog non–stationary signals. The second decomposer is for representing discrete non–stationary signals. It is based on a linear-chirp based transform that provides local time-frequency parametric representations based on linear chirps as intrinsic mode functions. Important applications of these procedures are the compression and processing of biomedical signals as it will be illustrated.**

***Index Terms*—Asynchronous signal processing; level–crossing sampling; asynchronous sigma delta modulators; time-frequency analysis; discrete linear chirp transform; non–stationary signals.**

I. Introduction

In most practical applications, signals under consideration are non–stationary. Conceptually, non–stationarity relates to the variation over time of the statistics of the signal. Thus the representation and processing of non–stationary signals is typically done assuming that the statistics either do not change with time (stationarity) or that remain constant in short time intervals (local stationarity). However, as Priestley [3] indicates: "... stationarity is a mathematical idealization that in some cases may be valid only as an *approximation* to the real situation." To consider the time–variability, non–stationary behavior needs to be connected to joint time–frequency spectral characterization even though the analysis is complicated by the inverse time and frequency relationship as set by the uncertainty principle [7], [23]. According to the Wold–Cramer representation [3], a non–stationary process can be thought of as the output of a time–varying system. As such, the distribution of the power of a non–stationary signal is a function of time and frequency [5], [6]. Therefore to process synchronously non–stationary signals, according to the Nyquist–Shannon sampling theory, it is necessary that they be sampled using a continuously varying sampling period. However, conventional synchronous processing assumes the signal being processed is band–limited and thus sampled uniformly with a sampling period that depends on the maximum frequency present in the signal. By ignoring that the frequency content is changing with time unnecessary samples are collected in regions where the signal is quiescent. A more appropriate approach would be to make the process signal–dependent.

Besides the signal–dependence of the processing, power consumption and type of processing are issues of great importance in many biomedical and sensor network applications that also need to be considered. In brain computer interfacing [19], for instance, the size of the devices, the difficulty in replacing batteries, possible harms to the patient from high frequencies generated by fast clocks, and the high power cost incurred in data transmission point to the need for asynchronous methodologies [10], [13], [15], [17], [22], and analog processing [16].

The Lebesgue sum, instead of the Riemann's sum used in uniform sampling, provides the rational for level–crossing (LC) sampling [15], [17], a signal–dependent approach. For a fixed set of quantization levels, the LC sampler acquires a sample whenever the signal coincides with one of those levels. Level–crossing sampling is independent of the Nyquist–Shannon band–limited signal constraint and has no quantization error in the amplitude. Although very efficient in the collection of significant data from the signal, LC sampling requires an *a priori* set of quantization levels and results in non–uniform sampling where for each sample we need to know not only the value of the sample but also the time at which it occurs. Selecting quantization levels that depend on the signal, rather than fixed levels, as is commonly done, is an issue of research interest [15], [24].

Although the signal–dependent strategy of LC sampling, akin to using signal sparseness in compressive sensing, provides an efficient sampling method for non–stationary signals it complicates the signal reconstruction. Reconstruction based on the Nyquits-Shannon's sampling theory (also attributed to

E. T. Whittaker and V. A. Kotelnikov) requires the signal to be band–limited. In practice, just like the assumption of stationarity, the band–limitedness condition on non–stationary signals is not appropriate: bandwidth is not an exact measure of the frequency content of a signal but rather a mathematical idealization, and the spectral representation of non–stationary signals is time–varying. Furthermore, Shannon's sinc interpolation for band–limited signals is not a well–posed problem. The sinc basis can be replaced by the prolate spheroidal wave (PSW) functions [1] having better time and frequency localization than the sinc function [11], [22]. The PSW functions allow more compression in the sampling [22], [28] and whenever the signal has band–pass characteristics, modulated PSW functions provide parsimonious representations [20], [25]. More importantly, the multi–level representation obtained through LC provides a way to process these analog signals digitally [16] — a desirable processing in many applications.

A different approach to sampling and reconstructing non–stationary signals, while satisfying the signal dependence and the low–power consumption, is possible using the Asynchronous Sigma Delta Modulator (ASDM) [13], [18]. The ASDM is a non–linear feedback system that maps a bounded analog signal into a binary signal with zero–crossing times that depend on the amplitude of the signal. It can be shown that the ASDM operation is an adaptive LC sampling scheme [24]. Moreover, using duty–cycle modulation we obtain a multi–level representation of an analog signal in terms of localized averages — computed in windows with supports that depend on the amplitude of the signal. Such representation allows us to obtain a signal decomposition that generalizes the Haar wavelet representation [26]. As we will show this is accomplished by latticing the time–frequency plane choosing fixed frequency ranges and allowing the time–windows to be set by the signal in each of these frequency ranges.

Synchronous processing is a special case of asynchronous processing. And thus, if the non–stationary signal is available as a sampled signal or as a discrete signal, one could use the localized processing. We have thus developed the Discrete Linear Chirp transformation (DLCT) [29] that compares well with the empirical mode decomposition (EMD) [9], [12], [30]. The EMD is a decomposition into intrinsic mode functions (IMFs) which satisfy a symmetry condition on their envelopes and the matching of their number of extrema and zero–crossings. Using the fact that generalized discrete chirp functions can be made to satisfy the IMF conditions, by decreasing the support locally linear chirps — instead of higher–order chirps — can be used to represent discrete non–stationary signals. The DLCT generalizes the Discrete Fourier transform (DFT) and can be used to obtain time–frequency representations of multi–component, discrete non–stationary signals just like the EMD, but using linear chirps as orthogonal basis functions as the IMFs.

Our main objective in this paper is to present, relate and develop further current techniques for asynchronous processing of non–stationary signals while pointing to their time–frequency framework. As such, we have organized the material as follows. In section II, we consider the Wold—Cramer spectral representation of non–stationary signals to highlight the time–varying nature of the statistics as well as the need to develop localized approaches for time–frequency representations. In section III, the non–uniform sampling required by the time–variation of the frequencies in non–stationary signals is presented. We then propose improvements on the sampling and reconstruction provided by LC samplers using the ASDM, resulting in a localized decomposition that generalizes the Haar wavelet representation of analog non–stationary signals. Finally, in section IV we consider a localized time–frequency approach for the decomposition of discrete non–stationary signals using the concept of the IMFs. We show that the local processing using generalizations of the Fourier transform approaches is possible and of great practical significance. Simulations are given to illustrate the main topic in each of the sections. Conclusions follow in section V.

II. Non–stationary Random Processes

To highlight the time–varying nature of the statistics of non–stationary signals and their time–frequency spectral representation, we briefly review the Wold–Cramer decomposition [3]. A non–stationary process $x(t)$ can be represented as the output of a linear, time–varying system with impulse response $h(t,\tau)$

$$x(t) = \int_{-\infty}^{\infty} h(t,\tau)\varepsilon(\tau)d\tau \tag{1}$$

where the white noise $\varepsilon(t)$, as a stationary process, is expressed in terms of sinusoids with random amplitudes and phases:

$$\varepsilon(t) = \int_{-\infty}^{\infty} e^{j\Omega t} dZ(\Omega) \tag{2}$$

and $Z(\Omega)$ is a random process with orthogonal increments:

$$E[dZ(\Omega_1)dZ^*(\Omega_2)] = 0 \qquad \Omega_1 \neq \Omega_2 \quad \text{and}$$
$$E[|dZ(\Omega)|^2] = \frac{d\Omega}{2\pi}.$$

Replacing (2) into (1), we can express the non–stationary process as

$$x(t) = \int_{-\infty}^{\infty} H(t,\Omega)e^{j\Omega t} dZ(\Omega) \qquad \text{where}$$
$$H(t,\Omega) = \int_{-\infty}^{\infty} h(t,\tau)e^{-j\Omega(t-\tau)}d\tau \tag{3}$$

is the generalized transfer function of the linear time–varying system. Given the above representation, the mean and variance of $x(t)$ are functions of time:

$$\eta_x(t) = \eta_\varepsilon \int_{-\infty}^{\infty} h(t,\tau)d\tau$$
$$E[|x(t) - \eta_x(t)|^2] = \frac{1}{2\pi}\int_{-\infty}^{\infty} |H(t,\Omega)|^2 d\Omega.$$

The Wold–Cramer evolutionary spectrum is defines as

$$S(t,\Omega) = |H(t,\Omega)|^2 \tag{4}$$

or the distribution of the power of the non–stationary process $x(t)$ at each time t as a function of the frequency Ω. This definition constitutes a special case of Priestley's evolutionary spectrum [3]. Instead of a class of oscillatory functions, as in Priestley's general case, the Wold–Cramer evolutionary spectrum is uniquely given by the representation of the non–stationary process. Estimators of the evolutionary spectrum are proposed in [5] and [6].

III. Non–uniform Sampling

Since the Wold–Cramer evolutionary spectrum changes continuously with time, to process discretely non–stationary signals requires, according to the Shannon–Nyquist theory, that they be sampled using a continuously varying sampling period. As such sampling using a uniform sampling period, determined by the highest frequency in the signal, is wasteful in the regions with low activity. Thus, two issues of interest are: how to sample and reconstruct non–stationary signals and how to decompose such signals following a time–frequency perspective. In this section we consider these issues.

A. Level Crossing Sampling and Reconstruction

A signal–dependent and efficient sampler, especially for signals sparse in time, is the level crossing (LC) sampler [17]. For a set of amplitude quantization levels $\{q_i\}$ an LC sampler (Fig. 1) acquires a sample whenever the amplitude of the signal coincides with one of the given quantization levels. This results in non–uniform sampling with more samples taken in regions where the signal has significant activity and fewer where the signal is quiescent. Although LC sampling requires the value of the sample and the time at which it occurs to be kept, it has the advantage that no band–limited constraint is required. From the sample values obtained by the LC sampler, the signal $x(t)$ is approximated by the multilevel signal

$$\hat{x}(t) = \sum_k q_k p_k(t) \tag{5}$$

for a unit pulse $p_k(t) = u(t - t_k) - u(t - t_{k+1})$, $t_{k+1} > t_k$, where $u(t)$ is the unit-step signal, and q_k the quantization level that coincides with $x(t_k)$. Typically the quantization levels are chosen uniformly, but better choices have been considered [17], [24].

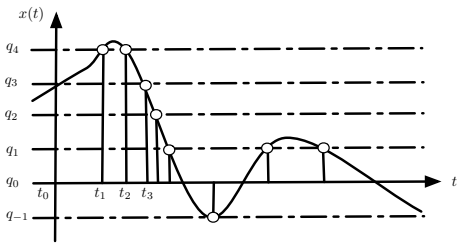

Fig. 1. Level-crossing sampler with uniform quantization levels.

To improve the multilevel approximation $\hat{x}(t)$, prolate spheroidal wave (PSW) functions $\{\phi_m(t)\}$ have been used [1], [11]. The advantage of using PSW functions is that among all the orthogonal bases defined in a time-limited domain $[-T, T]$, they have the maximum energy concentration within a given band of frequencies $(-W, W)$. These functions are eigenfunctions of the integral operator

$$\phi_n(t) = \frac{1}{\lambda_n} \int_{-T}^{T} \phi_n(x) S(t - x) dx \tag{6}$$

where $S(t)$ is the sinc function and $\{\lambda_n\}$ are the corresponding eigenvalues. Significantly, the sinc function $S(t)$ can be expanded in terms of the PSW basis $\{\phi_n(t)\}$ for a sampling period T_s as:

$$S(t - kT_s) = \sum_{m=0}^{\infty} \phi_m(kT_s)\phi_m(t) \tag{7}$$

allowing us to express Shannon's sinc interpolation in the following equivalent way:

$$x(t) = \sum_{m=0}^{\infty} \left[\sum_{k=-\infty}^{\infty} x(kT_s)\phi_m(kT_s) \right] \phi_m(t). \tag{8}$$

Now, if $x(t)$ has finite support $0 \le t \le (N-1)T_s$, a Fourier transform $X(\Omega)$, and is essentially band-limited in a frequency band $(-W, W)$, or equivalently the energy

$$\eta = \frac{1}{2\pi ||x||^2} \left[\int_{W}^{\infty} |X(\Omega)|^2 d\Omega + \int_{-\infty}^{-W} |X(\Omega)|^2 d\Omega \right] \;\rightarrow\; 0$$

outside this band, then $x(t)$ can be expressed as

$$x(t) = \sum_{m=0}^{M-1} \gamma_m \phi_m(t)$$
$$\text{where} \quad \gamma_m = \sum_{k=0}^{N-1} x(kT_s)\phi_m(kT_s) \tag{9}$$

for a value M chosen from the eigenvalues $\{\lambda_n\}$ that indicate the energy concentration. It is important to remark that given the connection with time and frequency used to obtain equation (9) it is a time–frequency representation of $x(t)$.

Now, we can represent $N_{\ell c}$ measurements $\{x(t_k)\}$, for non-uniform times $\{t_k,\ k = 0, \cdots, N_{\ell c} - 1\}$, acquired by an LC sampler, using PSW functions as

$$\mathbf{x}(\mathbf{t_k}) = \mathbf{\Phi}(\mathbf{t_k})\gamma_M \tag{10}$$

where $\mathbf{\Phi}(\mathbf{t_k})$ is an $N_{\ell c} \times M$ matrix —in general not square as typically $M < N_{\ell c}$— with entries $\{\phi_i(t_k)\}$ computed at the times $\{t_k\}$ in the vector $\mathbf{t_k}$. The expansion coefficients $\{\gamma_m\}$in the vector γ_M are found as

$$\gamma_M = \mathbf{\Phi}^{\dagger}(\mathbf{t_k})\mathbf{x}(\mathbf{t_k}) \tag{11}$$

where $\dagger$ indicates pseudo-inverse. Replacing the obtained coefficients in the top equation in (9) provides at best an approximation to the original signal. However, depending on the distribution of the time samples, the above problem could become ill-conditioned.

Regularization techniques [2], [4] are needed to obtain meaningful solutions of ill–conditioned problems. The Tikhonov

regularized solution of the measurement equation (10) can be posed as the mean–square minimization

$$\gamma_{M\,\mu} = \arg\min_{\gamma_M}\{\|\mathbf{\Phi}(\mathbf{t_k})\gamma_M - \mathbf{x}(\mathbf{t_k})\|^2 + \mu\|\gamma_M\|^2\} \qquad (12)$$

where the regularization parameter μ represents the tradeoff between losses and smoothness of the solution. Notice that if $\mu = 0$ the solution coincides with the pseudo-inverse solution (11). In general, the Tikhonov regularization decreases the effect of singular values smaller than μ. The optimal value for the regularization parameter μ is determined by *ad-hoc* methods [4], [28].

The regularized solution $\gamma_{M\,\mu}$ of (12) is given by

$$\gamma_{M\,\mu} = (\mathbf{\Phi}(\mathbf{t_k})^T\mathbf{\Phi}(\mathbf{t_k}) + \mu\mathbf{I})^{-1}\mathbf{\Phi}(\mathbf{t_k})^T\mathbf{x}(\mathbf{t_k}). \qquad (13)$$

To illustrate the LC sampling and the reconstruction using Tikhonov's regularization, consider a chirp signal being sampled with an LC sampler of fixed quantization values. Figure 2 displays the LC sampled signal, while Fig. 3 shows the reconstructed and the error signals using a regularization parameter $\mu = 10^{-4}$. Although the last segment of the signal is recovered, the initial part is not. This is in part due to the choice of quantization levels that are more suited for signals segments with larger amplitudes and higher frequencies.

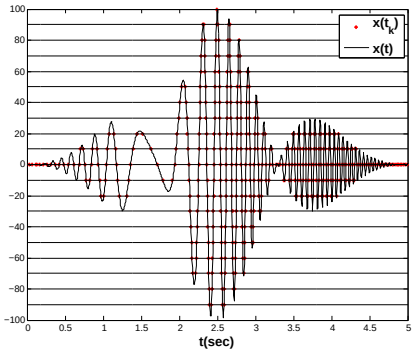

Fig. 2. Chirp signal being LC sampled using fixed quantization levels.

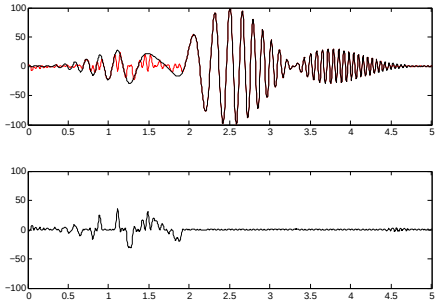

Fig. 3. Top: recovered signal using Tiknonov's regularization with $\mu = 10^{-4}$. Bottom: reconstruction error.

B. Asynchronous Sigma Delta Modulator Sampling and Reconstruction

The LC technique has three main drawbacks: (i) requiring both amplitude and time for each of the samples, (ii) selecting appropriate quantization levels, and (iii) lacking a reconstruction error measure. In this section we show that sampling and reconstruction using an asynchronous sigma delta modulator (ASDM) [24] improve on these three issues. An ASDM [13] is a nonlinear feedback system that operates at low power and consists of an integrator and a Schmitt trigger (see Fig. 4). It has been used to time encode a bounded and band–limited analog signal into a continuous-time signal with binary amplitude [13].

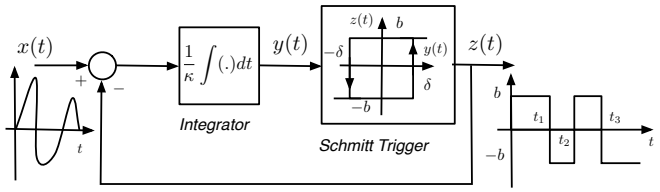

Fig. 4. Asynchronous Sigma Delta Modulator

For a bounded signal $x(t)$, $|x(t)| \leq c$, and an appropriate value of the ASDM scale parameter κ, the ASDM maps the amplitude of $x(t)$ into a binary signal $z(t)$ of amplitude $\pm b$. If in $t_k \leq t \leq t_{k+1}$ the output of the Schmitt trigger is the binary signal $z(t) = b(-1)^{k+1}[u(t-t_k) - u(t-t_{k+1})]$ where $u(t)$ is the unit–step function and $b > c$, the output of the integrator $y(t)$ is bounded, i.e., $|y(t)| < \delta$. Thus, the difference $y(t_{k+1}) - y(t_k) = \pm 2\delta$ is equal to

$$\frac{1}{\kappa}\left[\int_{t_k}^{t_{k+1}} x(\tau)d\tau - (-1)^{k+1}b(t_{k+1}-t_k)\right]$$

and gives the integral equation [13]:

$$\int_{t_k}^{t_{k+1}} x(\tau)d\tau = (-1)^k[-b(t_{k+1}-t_k) + 2\kappa\delta]. \qquad (14)$$

Thus the amplitude information of $x(t)$ is now related to the duration of the pulses in $z(t)$ or equivalently to the zero–crossing times $\{t_k\}$. Moreover, approximating the integral equation (14) gives an approximation of the signal using the zero–crossing times [18].

For band–limited signals, perfect reconstruction from non–uniform samples can be attained provided that the zero–crossing times $\{t_k\}$ satisfy the condition [13]:

$$\max_k(t_{k+1} - t_k) \leq T_N$$

where $T_N \leq 1/2f_{max}$ is the Nyquist sampling period for a band–limited signal with maximum frequency f_{max}. Thus, using equation (14) we obtain

$$\frac{2\kappa\delta}{b+c} \leq t_{k+1} - t_k \leq \frac{2\kappa\delta}{b-c} \leq T_N \qquad (15)$$

which gives a way to choose the scale parameter κ in terms of the Nyquist sampling rate. Letting $\delta = 0.5$ we have

$$\kappa \leq T_N(b-c) \leq \frac{b-c}{2f_{max}} \qquad (16)$$

indicating the scale parameter κ depends not only on the maximum frequency of the signal but on the difference in amplitude of the signal, c, and the choice of b.

The sequence of binary rectangular pulses $z(t)$ is characterized by the duty-cycle $0 < \alpha_k/T_k < 1$ of two consecutive pulses of duration $T_k = \alpha_k + \beta_k$ where $\alpha_k = t_{k+1} - t_k$ and $\beta_k = t_{k+2} - t_{k+1}$. Letting

$$\zeta_k = \frac{\alpha_k - \beta_k}{\alpha_k + \beta_k}$$

we have that the duty cycle $\alpha_k/T_k = (1 + \zeta_k)/2$ where, as shown next, ζ_k is the local average of $x(t)$ in $t_k \le t \le t_{k+1}$. Indeed, the integral equation (14) can be written in terms of $z(t)$ as

$$\int_{t_k}^{t_{k+1}} x(\tau)d\tau = (-1)^{k+1} \int_{t_k}^{t_{k+1}} z(\tau)d\tau + 2(-1)^k \kappa\delta$$

which can be used to get local estimate of the signal average ζ_k in $[t_k,\ t_{k+2}]$:

$$\frac{1}{T_k}\int_{t_k}^{t_{k+2}} x(\tau)d\tau \quad = \quad \frac{(-1)^{k+1}}{T_k}\left[\underbrace{\int_{t_k}^{t_{k+1}} z(t)dt}_{\alpha_k} - \underbrace{\int_{t_{k+1}}^{t_{k+2}} z(t)dt}_{\beta_k}\right]$$

where as indicate above $T_k = t_{k+2} - t_k = \alpha_k + \beta_k$.

Thus, for a bounded and band-limited analog signal the corresponding scale parameter determines the width of an appropriate window — according to the non–uniform zero–crossing times — to compute an estimate of the local average. Thus, the ASDM provides either a binary representation of its input $x(t)$ by its binary output $z(t)$ and the integral equation, or a sequence of local averages $\{\zeta_k\}$ at non–uniform times $\{t_{2k}\}$. Different from the LC sampler, the ASDM only requires the sample times, the quantization levels are set by the amplitude of the signal. The main drawback of this approach, however, is the condition that the input signal be band–limited so as to obtain a value for κ. A possible alternative to avoid this is to lattice the time–frequency plane by arbitrary frequency windows and for the signal component in each of these ranges to have arbitrary time windows according to their amplitude. This results in an asynchronous decomposition which we discuss next.

C. ASDM–based Decomposition for Analog Signals

The local–average approximation obtained above for a scale parameter κ of the ASDM is similar to the Haar wavelet representation [8] but with the distinction that the time–windows are signal–dependent instead of being fixed. Indeed, it is possible to generate pulses with duty–cycle determined by the sequence $\{\alpha_k,\ \beta_k\}$. Indeed, if $\nu(t) = u(t) - u(t-0.5)$ is a scaling function the wavelet function can be defined as

$$\psi_{\alpha_k,\beta_k,t_k,t_{k+1}}(t) = \nu\left(\frac{0.5t}{\alpha_k} - t_k\right) - \nu\left(\frac{0.5t}{\beta_k} - t_{k+1}\right)$$

So that local averages are found as

$$\zeta_k = \frac{1}{t_{k+2} - t_k}\int_{t_k}^{t_{k+2}} \psi_{\alpha_k,\beta_k,t_k,t_{k+1}}(t)z(t)dt \tag{17}$$

giving an approximation for $x(t)$ similar to the one given by a wavelet representation:

$$\hat{x}(t) = \sum_{k \text{ even}} \zeta_k p_k(t) \tag{18}$$

for unit pulse $p_k(t) = u(t - t_k) - u(t - t_{k+2})$. This is a generalization of the Haar wavelet [8] for a particular value of the scale κ. As such, our representation has the properties of wavelet representations.

For a scale parameter κ for the ASDM, the resulting set of local averages $\{\zeta_k\}$ — depending on the zero–crossing times $\{t_k\}$ or $\{\alpha_k, \beta_k\}$ — provide the multi–level approximation (18) of $x(t)$. Considering that ζ_k is the best mean–square estimator of the signal in $[t_k, t_{k+2}]$ when no data is provided, the ASDM can be thought of an optimal LC sampler. More importantly, using different values of κ allows us to obtain different scale representations of the signal.

The scale decomposition is obtained by latticing the time–frequency plane so that the frequency axis is segmented to obtain related scale parameters κ_ℓ, and the time axis is divided according to the width of the different time–windows determined by the scale parameters. For instance, to obtain a set of scales

$$\kappa_\ell = \frac{\kappa_1}{2^{\ell-1}} \qquad \ell = 2, \cdots, L$$

we would choose a narrow–band low–pass filter with bandwidth f_1 such that $\kappa_1 = (b - c)/f_1$ according to (16), and for the next modules we would choose low–pass filters of bandwidths $2^{\ell-1}f_1$ (Hz), $\ell = 2, \cdots, L-1$, i.e., it is doubled at each module after the first to cover the bandwidth of the input signal. This is the equivalent of anti–aliasing filtering in the Shannon-Nyquist sampling theory. These scale low–pass filters allow us to obtain appropriate scale parameters for the ASDMs in the decomposer.

The decomposer consists of L cascaded modules, each having a scale low–pass filter, an ASDM, an averager, a smoothing low-pass filter and an adder. Figure 5 shows two modules of the decomposer. The number of modules, L, is determined by the range of frequencies of interest in the signal. For a certain scale κ_ℓ, determined by the maximum cutoff frequency of the corresponding scale filter, the ASDM maps the input signal into a sequence $\{\alpha_{k,\ell}, \beta_{k,\ell}\}$ which the averager converts into local averages $\{\zeta_{k,\ell}\}$. The smoothing low-pass filter, after the averager, is used to avoid discontinuities that may occur when the multi-level signal $d_\ell(t)$ is subtracted from the input signal of the corresponding module. Each of these modules operates similarly but at a different scale.

The input to the modules beyond the first one can be written

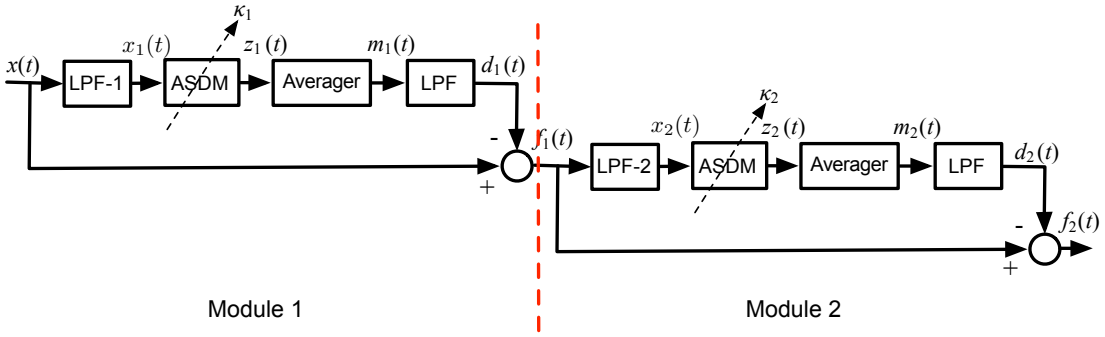

Fig. 5. Two module ASDM–based decomposer: a bounded analog non–stationary signal $x(t)$ is the input, $\{d_\ell(t)\}$ are the multi–level low–frequency components, and $\{f_\ell(t)\}$ the residual signals.

sequentially as follows,

$$\begin{aligned} f_1(t) &= x(t) - d_1(t) \\ f_2(t) &= f_1(t) - d_2(t) = x(t) - d_1(t) - d_2(t) \\ &\vdots \\ f_L(t) &= x(t) - \sum_{\ell=1}^{L} d_\ell(t). \end{aligned} \tag{19}$$

We thus have the decomposition

$$x(t) = \sum_{\ell=1}^{L} d_\ell(t) + f_L(t) \approx \sum_{\ell=1}^{L} \sum_{k} \zeta_{k,\ell}\ p_k(t) + f_L(t) \tag{20}$$

where the $\{d_\ell(t)\}$ are the low–frequency components of $x(t)$ and of $\{f_k(t)\}$, $f_L(t)$ can be thought of as the error of the decomposition and as before $p_k(t) = u(t - t_k) - u(t - t_{k+2})$. The averages $\{\zeta_{k,\ell}\}$ depend on the scale being used and computed as in (17). This scale decomposition is analogous to a wavelet decomposition for continuous signals.

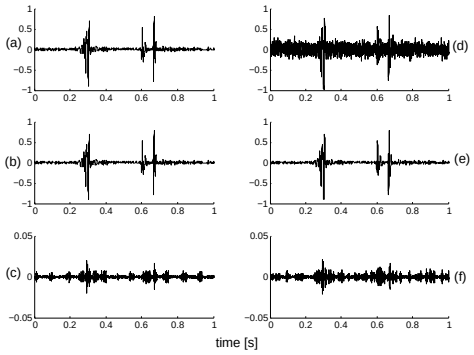

Fig. 6. Left: phonocardiogram recording of a heart sound without noise (a); reconstructed signal (b); and reconstruction error (c). Right: phonocardiogram recording with additive noise (d); reconstructed signal (e); and reconstruction error (f).

To illustrate the performance of the decomposer we consider a phonocardiogram recording of a heart sound, shown on the top left of Fig. 6, and interpolated to approximate an analog signal in the simulation. In Figs. 6 and 7, we display the reconstruction of the original with and without additive noise. Similar to a wavelet representation, the decomposition algorithm is robust to additive, zero–mean noise. The reconstructed signal in both cases are very similar. For the noise–free recording, Fig. 8 displays the multilevel signals d_i, $i = 1, 2$. The histograms on the right side of the figure show the prevalence of some averages. Selecting the most prevalent averages and the corresponding zero–crossing $[t_k,\ t_{k+2}]$ provide a compressed representation of the signal.

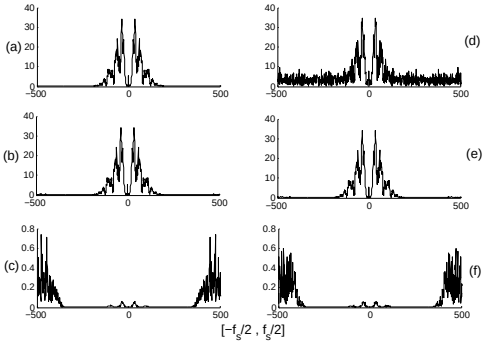

Fig. 7. Left: spectra of phonocardiogram recording of a heart sound without noise (a); of the reconstructed signal (b); and of the reconstruction error (c). Right: spectra of phonocardiogram recording of a heart sound with additive noise (d); of the reconstructed signal (e); and of the reconstruction error (f).

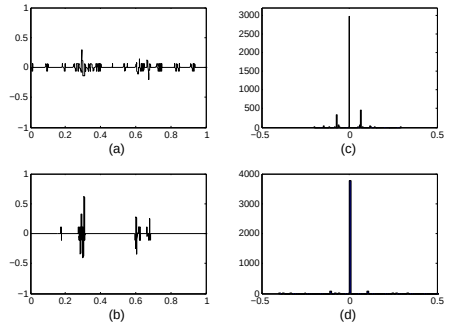

Fig. 8. Multilevel signal components for noiseless recording, (a) and (b); histograms of the averages for the components, (c) and (d).

IV. Linear–Chirp Decomposition

Synchronous sampling is a special case of asynchronous sampling. As such, according to equations (14) and (16), letting $\delta = 0.5$, the ASDM scale parameter that would give uniform sampling with a sampling period $T_N = t_{k+1} - t_k$

satisfying the Nyquist conditions is

$$\kappa_k = (-1)^k \int_0^{T_N} x(\tau + kT_N)d\tau + bT_N \quad \text{and}$$
$$|\kappa_k| \leq \frac{b-c}{2f_{max}}, \qquad k = 0, 1, \cdots \tag{21}$$

clearly indicating the dependence of the scale parameter on the amplitude as well as on the maximum frequency of the signal. Although using an ASDM for uniform sampling might not be a practical approach, the above suggests that amplitude as well as frequency need to be considered in the sampling process. In this section, we will explore the local processing used before for uniformly sampled or discrete non–stationary signals.

Intrinsic mode functions (IMFs), i.e., functions with a point–wise zero–mean envelop and matching extrema and zero–crossings, are the basis for the empirical mode decomposition (EMD) [9], [30]. Although the EMD does not attempt to optimize an error criteria or to use orthogonal basis functions, it is in most cases an efficient signal–dependent and intuitive approach to represent non–stationary signals. The EMD is connected through the Hilbert transform to a time-frequency spectrum, the Hilbert spectrum, where the instantaneous frequency of each of the components is obtained [12], [21].

A finite–support chirp function

$$c(t) = Ae^{j\phi(t)} \qquad 0 \leq t \leq T \quad \text{where}$$
$$\phi(t) = \Omega_0 t + \sum_{n=1}^{N} \beta_n t^{n+1}$$

with the duration T adjusted, so that the extrema and the number of zero crossings match, constitutes an IMF. Decreasing the support of the chirp we could consider linear chirps rather than higher–order chirps to obtain a local representation. In [29] we have proposed a local signal representation using linear chirps, or the discrete linear chirp transform (DLCT). Such a transformation is an extension of the DFT and provides a local IMF decomposition for discrete non–stationary signals. For $x(n)$, $0 \leq n \leq N-1$, we obtain a decomposition

$$x(n) = \sum_{\ell=-L/2}^{L/2-1} \sum_{k=0}^{N-1} \frac{X(k,\ell)}{LN} \exp\left(j\frac{2\pi}{N}(\ell C n^2 + kn)\right)$$
$$0 \leq n \leq N-1, \quad C = 2\Lambda/L \tag{22}$$

where the chirp–rate is discretized to a finite domain $[-\Lambda,\ \Lambda]$ with resolution $1/L$, and

$$X(k,\ell) = \sum_{n=0}^{N-1} x(n) \exp\left(-j\frac{2\pi}{N}(\ell C n^2 + kn)\right),$$
$$0 \leq k \leq N-1, \quad -\frac{L}{2} \leq \ell \leq \frac{L}{2} - 1. \tag{23}$$

It is important to notice that $X(k,0)$ is the DFT of $x(n)$, and that different from the Hilbert spectrum the DLCT provides a parametric representation of the instantaneous frequency of each of the signal components. The parameters can be obtained from the peaks of the magnitude square $|X(k,\ell)|^2$ connected with the energy distribution of the signal.

To illustrate the decomposition with the DLCT, consider the uniformly sampled speech segment shown in Fig. 9(a). Such a signal is decomposed into the five components $\{s_i(n)\}$ shown in Fig. 10 along with their spectra. Notice these five components display the characteristics of IMFs and that the first four display no frequency overlap due to the orthogonality of the basis. Using these five components a reconstruction of the signal and its error are shown in Fig. 9(b) and (c).

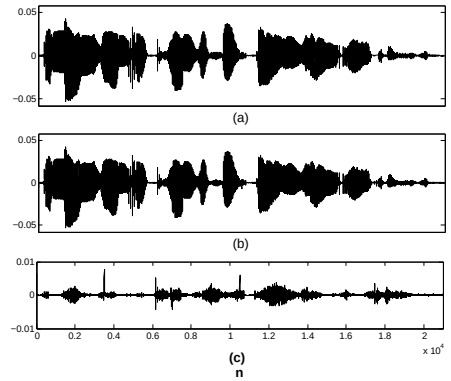

Fig. 9. Original uniformly sampled speech segment (a); reconstructed signal using 5 components (b); and (c) reconstruction error.

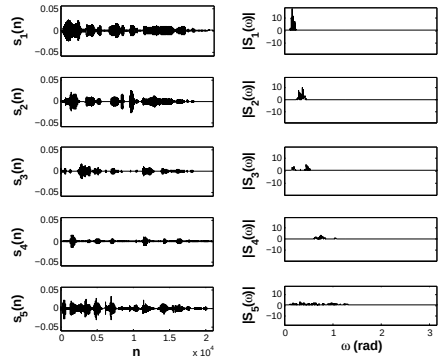

Fig. 10. Five components of the speech segment and their corresponding spectra.

V. Conclusion

Since non–stationary signals result from so many applications, their representation and processing are issues of great research interest. In this paper, we have provided a comprehensive discussion of the asynchronous processing of non–stationary signals within a time–frequency framework. Two decomposition procedures were considered. One is based on the ASDM for analog non–stationary signals and it generalizes the Haar wavelet representation. The other is intended for discrete non–stationary signals and is based on a local time–frequency representation using chirps as intrinsic mode functions. Simulations with actual signals illustrate the decomposition algorithms for representation and compression applications. Further research is being conducted to study these two decomposition methods and their use in practical application in biomedicine and communications.

VI. AUTHORS

Luis F. Chaparro (chaparro@ee.pitt.edu) received his PhD in electrical engineering from the University of California, Berkeley. He is currently an Associate Professor in the Department of Electrical and Computer engineering of the University of Pittsburgh, PA. He served as associate editor of the IEEE Signal Processing and of the Journal of the Franklin Institute, and is a senior member of IEEE. His research interest is in statistical signal processing and time–frequency analysis for application in biomedical engineering and communications.

Ervin Sejdic(esejdic@pitt.edu) received his PhD degree in electrical engineering from the University of Western Ontario, Canada. He was a Postdoctoral Fellow at Holland Bloorview Kids Rehabilitation Hospital/University of Toronto and a Research Fellow at Beth Israel Deaconess Medical Center/Harvard Medical School. He is currently Assistant Professor at the department of electrical and computer engineering, University of Pittsburgh. His research interests are in biomedical engineering and signal processing.

Azime Can (azc9@pitt.edu) is currently a PhD candidate in the Department of Electrical and Computer Engineering at the University of Pittsburgh. Her research interests are in signal processing and coding with applications in biomedical, neuroscience and wireless communications.

Osama A. Alkishriwo (alkishriewo@yahoo.com) is currently a PhD candidate in the Department of Electrical and Computer Engineering at the University of Pittsburgh. His research interest are in wireless communications, time-frequency analysis, and compressive sensing.

Seda Senay (ssenay@ucmerced.edu) received her PhD degree in electrical engineering from the University of Pittsburgh. Currently, she is a postdoctoral researcher at the University of California, Merced, working on signal and image recovery methods from compressive measurements. Her research interests are in sampling theory and time-frequency methods.

Aydin AKAN (akan@istanbul.edu.tr) received hid Ph.D. degree in electrical engineering from the University of Pittsburgh. He is with the Department of Electrical and Electronics Engineering, University of Istanbul. His current research interests are time-frequency analysis with application to wireless communications and bioengineering. He is a senior member of IEEE and associate editor of the Digital Signal Processing Journal.

REFERENCES

[1] D. Slepian and H. Pollak, "Prolate spheroidal wave functions, Fourier analysis and uncertainty" *Bell System Tech. J.*, vol. 40, pp. 43–64, 1961.

[2] A. N. Tikhonov, "Solution of incorrectly formulated problems and the regularization method," *Soviet Math. Dokl.*, vol. 4, pp. 1035–1038, 1963.

[3] M. B. Priestley, *Spectral Analysis and Time Series.* Academic Press., London, 1981.

[4] P. Hansen and D. P. Oleary, "The use of L–curve in the regularization of discrete ill–posed problems," *SIAM J. Sci. Compt.*, vol. 14, pp. 1487–1503, 1993.

[5] A.S. Kayhan, A. El–Jaroudi, and L.F. Chaparro, "Evolutionary periodogram for nonstationary signals," *IEEE Transactions on Signal Processing,* vol. 42, pp. 1527 –1536, Jun. 1994.

[6] A.S. Kayhan, A. El–Jaroudi, and L.F. Chaparro, "Data–adaptive evolutionary spectral estimation," *IEEE Transactions on Signal Processing*, vol. 43, pp. 204 – 213, Jan. 1995.

[7] L. Cohen, *Time–frequency Analysis: Theory and Applications.* Prentice-Hall, New York, 1995.

[8] G. Strang and T. Nguyen, *Wavelets and Filter Banks.* Wellesly–Cambridge Press, Wellesly, MA, 1997.

[9] N. Huang, Z. Shen, S. Long, M. Wu, H. Shih, Q. Zheng, N. Yen, C. Tung, and H. Liu, "The empirical mode decomposition and Hilbert spectrum for nonlinear and nonstationary time series analysis," *Proc. Roy. Soc. London A*, vol. 454, pp. 903–995, Mar. 1998.

[10] F. Marvasti, *Nonuniform Sampling: Theory and Practice*. Kluwer Academic/Plenum Publishers, New York, 2001.

[11] G. Walter, X. Shen, "Sampling with prolate spheroidal wave functions," *Sampling Theory in Sig. and Image Proc.*, vol. 2, pp. 25–52, Jan. 2003.

[12] P. Flandrin, G. Rilling, and P. Goncalves, "Empirical mode decomposition as a filter bank," *IEEE Signal Proc. Letters*, vol. 11, pp. 112–114, Feb. 2004.

[13] A. Lazar and L. Toth, "Perfect recovery and sensitivity analysis of time encoded bandlimited signals," *IEEE Trans. Circ. and Syst.*, vol. 51, pp. 2060–2073, Oct. 2004.

[14] G. Walter and X. Shen, "Wavelets based on Prolate Spheroidal Wave functions," *J. of Fourier Anal. and Appls.*, vol. 10, 2004.

[15] K. Guan and A. Singer, "A Level-crossing sampling scheme for non-bandlimited signals," *IEEE Intl. Conf. Acoustics, Speech and Signal Proc.,* vol. III, pp. 381–383, 2006.

[16] Y. Tsividis, "Mixed-domain systems and signal processing based on input decomposition," *IEEE Trans. Circuits and Syst.*, vol. 53, pp. 2145–2156, Oct. 2006.

[17] K. Guan, S. Kozat and A. Singer, "Adaptive reference levels in a level-crossing analog-to-digital converter," *EURASIP J. Advances in Sig. Proc.,* vol. 2008, doi:10.1155/2008/513706.

[18] A. Lazar, E. Simonyi and L. Toth, "An overcomplete stitching algorithm for time decoding machines," *IEEE Trans. Circuits and Systems –I,* vol. 55, pp. 2619–2630, Oct. 2008.

[19] Pathway to the Mind — Brain–Computer Interfaces, *IEEE Signal Processing Magazine,* vol. 25, Jan. 2008.

[20] E. Sejdić, M. Luccini, S. Primak, K. Baddour, and T. Willink, "Channel estimation using DPSS based frames," *IEEE Intl. Conf. Acoust., Speech and Sig. Proc.*, pp. 2849–2852, Mar. 2008.

[21] C. Lai, R. Narayanan, Q. Ruan, and A. Davydov, "Hilbert-Huang transform analysis of human activities using through-wall noise and noise-like radar," *IET Radar, Sonar Navigation*, vol. 2, pp. 244-255, 2008.

[22] S. Şenay, L. Chaparro, L. Durak, "Reconstruction of non–uniformly sampled time-limited signals using prolate spheroidal wave functions," *Sig. Proc.,* vol. 89, pp. 2585–2595, 2009.

[23] E. Sejdić, I. Djurović, J. Jiang, "Time-frequency feature representation using energy concentration: An overview of recent advances, *Digital Sig. Proc.*, vol. 19, pp. 153–183, Jan. 2009.

[24] S. Şenay, L. F. Chaparro, M. Sun, and R. Sclabassi, "Adaptive level–crossing sampling and reconstruction," *European Signal Proc. Conf.,* pp. 1296–1300, 2010.

[25] J. Oh, S. Şenay, and L. F. Chaparro, "Signal Reconstruction from nonuniformly spaced samples using Evolutionary Slepian Transform-based POCS," *EURASIP J. Advances Sig. Proc.,* vol. 2010, doi:10.1155/2010/367317.

[26] Can, A., Sejdić, E., and Chaparro, L.F., " An asynchronous scale decomposition for biomedical signals," *IEEE Sig. Proc. in Medicine and Biol. Symp.*, pp. 1–6, 2011.

[27] E. Sejdić, A. Can, L. F. Chaparro, C. Steele, and T. Chau, "Compressive sampling of swallowing accelerometry signals using time-frequency dictionaries based on modulated discrete prolate spheroidal sequences," *EURASIP J. Advances Sig. Proc.*, vol. 101, doi:10.1186/1687-6180-2012-101.

[28] S. Şenay, J. Oh, and L. F. Chaparro, "Regularized signal reconstruction for level-crossing sampling using Slepian functions," *Signal Processing*, vol. 92, pp. 1157–1165, 2012.

[29] O. A. Alkishriwo and L. F. Chaparro, "A discrete linear chirp transform (DLCT) for data compression," *IEEE Intl. Conf. Info. Science, Sig. Proc. and Applic.,* pp. 1283–1288, Jul. 2012.

[30] X. Hu, S. Peng, and W. Hwang, "EMD revisited: a new understanding of the envelope and resolving the mode–mixing problem in AM–FM signals," *IEEE Trans. Signal Processing,* vol. 60, pp. 1075–1086, Mar. 2012.